

Solid ↔ liquid phase transformations in hypereutectic P/M Al-Si-Fe-X alloys

G. TIMMERMANS, L. FROYEN, J. VAN HUMBEECK
 Department Metaalkunde en Toegepaste Materiaalkunde (MTM),
 Katholieke Universiteit Leuven, Belgium

In this study, the metastable and stable solid ↔ liquid phase transformations of the hypereutectic alloys Al-20Si-5Fe-2Ni (wt%) and Al-17Si-5Fe-3.5Cu-1.1Mg-0.6Zr in as-atomised powder and in as-hot-forged material have been investigated. Differential Scanning Calorimetry (DSC) measurements at high temperatures have been performed. The resultant products have been thoroughly analysed using Light Optical Microscopy (LOM), Scanning Electron Microscopy (SEM) and Energy Dispersive Spectroscopy (EDS) microanalysis. During solidification large Si, δ (Al₄FeSi₂), FeNiAl₉, Al₇Cu₂Fe and Q(Cu₂Mg₈Si₆Al₅) are formed. A cooling rate of 5 °C/min and 1 °C/min is too high for the formation of the equilibrium phases β (Al₅FeSi) and Al₇Cu₂Fe. The understanding of the sequence of transformations is useful in order to define appropriate processing parameters for these alloys produced by powder metallurgy. The temperature at which the first liquid phase appears during heating at 5 °C/min is 559 °C for the Al-Si-Fe-Ni powder and 506 °C for the Al-Si-Fe-Cu-Mg-Zr powder. © 2000 Kluwer Academic Publishers

1. Introduction

The aim of this study is to identify the temperature at which the first liquid appears and the (metastable or stable) solid ↔ liquid phase transformations in the powder metallurgical (P/M) Al-Si-Fe-X alloys. As-atomised powder and hot forged material of Al-20Si-5Fe-2Ni (wt%) (alloy A) and Al-17Si-5Fe-3.5Cu-1.1Mg-0.6Zr (alloy B) are investigated. Hypereutectic Al-Si-alloys produced by P/M are known to have excellent properties suitable for application in the transport sector, mainly due to their low density, very fine microstructure resulting in good mechanical properties, high wear resistance and thermal conductivity and low coefficient of thermal expansion. Final consolidation after cold compacting of the alloyed powder can be done by hot extrusion, hot isostatic pressing or by hot forging, which can be applied as a near-net-shaping technique. Spray forming as a consolidation technique has also been reported [1–3].

In literature, very little information is available concerning the solid ↔ liquid phase transformations of these alloys. Most important among these are the work on the Al-Fe-Si system by Rivlin and Raynor [4] and Petrova *et al.* [5], and that on the transformations and phases in various systems reported by Mondolfo [6]. The knowledge of the solid ↔ liquid phase transformations is necessary in order to choose appropriate hot forming and heat treatment temperatures. Since these P/M alloys are shaped by near-net-shaping processes, the dimensions of a part have to be predictable. Incipient melting or decomposition of phases during thermomechanical processing should therefore be avoided or at least minimised. This is also necessary to avoid shrinkage porosity and formation of brittle phases. Samuel

et al. [7] observed that melting of the Al₂Cu phase during solution heat treatment of Al-6.2Si-3.2Cu-0.15Fe alloy was detrimental to the tensile properties. On the other hand, Narayanan *et al.* [8] found that the tensile properties of the alloy Al-6.2Si-3.2Cu-0.3Mg-0.15Fe with increased Fe content are improved by partial melting, but only if the solution temperatures are moderate (515–520 °C), in order to avoid the formation of too much liquid. The reason of the success of partial melting is the elimination of β (Al₅FeSi) platelets by partial dissolution, fragmentation and spheroidisation, eliminating the negative effect of this phase. In addition, a more efficient dissolution of Al₂Cu occurs so that more Cu is dissolved in the Al matrix which precipitates during subsequent ageing, leading to an increase in the strength.

2. Experimental

The investigated Al-Si-Fe-Ni and Al-Si-Fe-Cu-Mg-Zr powders (designated alloy A and alloy B respectively) were gas atomised (N₂ + O₂) at Eckart-Werke (Germany). Cold compacted powder was forged at 490 °C and investigated in the as-forged condition. Non-isothermal heat treatments (thermal cycles) were performed on powder and on forged material using Differential Scanning Calorimetry (DSC) (Netch 404 calorimeter). The typical mass of a sample was about 20–60 mg, and the sample was placed in an alumina crucible in argon atmosphere. Two subsequent identical heating-cooling cycles were applied to reveal eventual metastable transformations. The thermal cycle consisted of heating from room temperature to 750 °C at

TABLE I Details of the phase transformations occurring in powder and forged (*temperatures in italic*) alloy A (Al-20Si-5Fe-2Ni) for two subsequent thermal cycles at 5 °C/min

Thermal cycle 1		Thermal cycle 2		Type
<i>T</i> (°C)	Reaction	<i>T</i> (°C)	Reaction	
Heating				
559, <i>560</i>	Al + Si + β + Ni-precip. \rightarrow L	555, <i>556</i>	Al + Si + δ + FeNiAl ₉ \rightarrow L	Eutectic Quasi-peritectic
589, <i>589</i>	β + Si \rightarrow L + δ			
Cooling				
710, <i>713</i>	L \rightarrow δ , L \rightarrow δ + Si	707, <i>712</i>	L \rightarrow δ , L \rightarrow δ + Si	Eutectic
550, <i>556</i>	L \rightarrow Al + Si + δ + FeNiAl ₉	553, <i>555</i>	L \rightarrow Al + Si + δ + FeNiAl ₉	

TABLE II Details of the phase transformations occurring in powder and forged (*temperatures in italic*) alloy B (Al-17Si-5Fe-3.5Cu-1.1Mg-0.6Zr) for two subsequent thermal cycles at 5 °C/min; Q = Cu₂Mg₈Si₆Al₅

Thermal cycle 1		Thermal cycle 2		Type
<i>T</i> (°C)	Reaction	<i>T</i> (°C)	Reaction	
Heating				
505, <i>506</i>	Decomposition of Al ₇ Cu ₂ Fe	497, <i>497</i>	Decomposition of Al ₂ Cu	Eutectic
519, <i>518</i>	Decomposition of Q	508, <i>508</i>	Decomposition of Al ₇ Cu ₂ Fe	
545, <i>545</i>	Al + Si + β + Cu-, Mg-precipitates \rightarrow L	520, <i>519</i>	Decomposition of Q	
584, <i>585</i>	β + Si \rightarrow L + δ , involving Cu-, Mg-rich phases	544, <i>544</i>	Al + Si + δ/β + Cu-, Mg-precipitates \rightarrow L	Quasi-peritectic
Cooling				
698, <i>697</i>	L \rightarrow δ , L \rightarrow δ + Si	695, <i>693</i>	L \rightarrow δ , L \rightarrow δ + Si	Quasi-peritectic
596, <i>599</i>	L + δ \rightarrow β + Si, involving Cu-,Mg-rich phases	596, <i>598</i>	L + δ \rightarrow β + Si, involving Cu-, Mg-rich phases	
546, <i>542</i>	L \rightarrow Al + Si + δ/β + Cu-, Mg-rich phases	546, <i>543</i>	L \rightarrow Al + Si + δ/β + Cu-, Mg-rich phases	Eutectic
514, <i>513</i>	Formation of Q	509, <i>510</i>	Formation of Q	Eutectic
490, <i>490</i>	Formation of Al ₂ Cu	489, <i>490</i>	Formation of Al ₂ Cu	

5 °C/min, holding for 15 min at 750 °C, followed by cooling to room temperature at 5 °C/min or 1 °C/min. Microstructural changes were studied using Light Optical Microscopy (LOM), Scanning Electron Microscopy (SEM) and Energy Dispersive Spectroscopy (EDS) microanalysis using an electron microprobe.

3. Results and discussion

An overview of the occurring phase transformations during heating and cooling of the powder and forged alloys is given in Tables I and II, together with the corresponding transformation temperatures.

3.1. Atomised powder Al-20Si-5Fe-2Ni (Alloy A)

The DSC measurements of as-atomised powder of alloy A (Fig. 1) are very reproducible (identical curves were obtained from 3 different samples). In the following, the transformations are given as a function of the onset temperature. Some of these transformations could only be identified using the accompanying microstructural investigations (including microanalysis).

The starting powder microstructure is very fine and contains primary and eutectic Si particles in a supersaturated Al(Si) matrix; the plate-like metastable δ (Al₄FeSi₂) phase appears mostly as needles in the section, and some small Ni-rich precipitates are found on the surface of the δ needles, as shown in (Fig. 2).

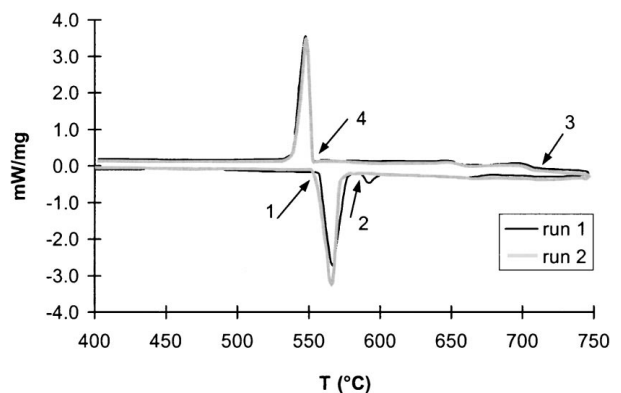


Figure 1 DSC curves of the first and second thermal cycle of powder A (Al-20Si-5Fe-2Ni).

The solid state transformations during the heating part of the first thermal cycle have been defined previously by Timmermans and Froyen [9, 10] as: Si-precipitation (200–300 °C), full transformation from metastable δ (Al₄FeSi₂) to the stable β (Al₅FeSi) between 300–400 °C, and the growth of Ni-rich precipitates from 300 °C upwards. In that study, the solid state transformations were identified employing low temperature DSC measurements and isothermal annealing experiments, combined with LOM, SEM, microanalysis (EDS) and X-ray Diffractometry (XRD).

During the first heating cycle, the measured eutectic temperature is 559 °C (peak 1 in Fig. 1) and corresponds

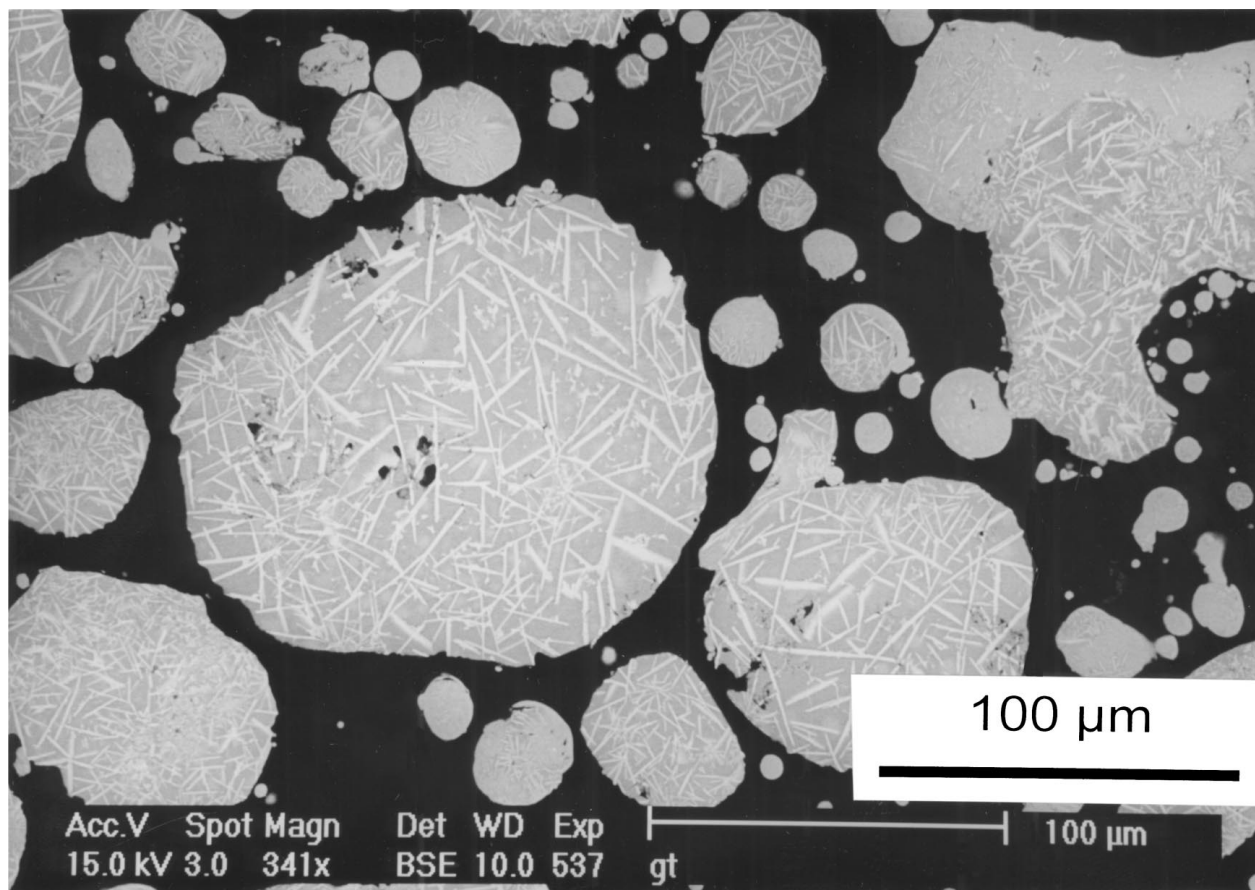


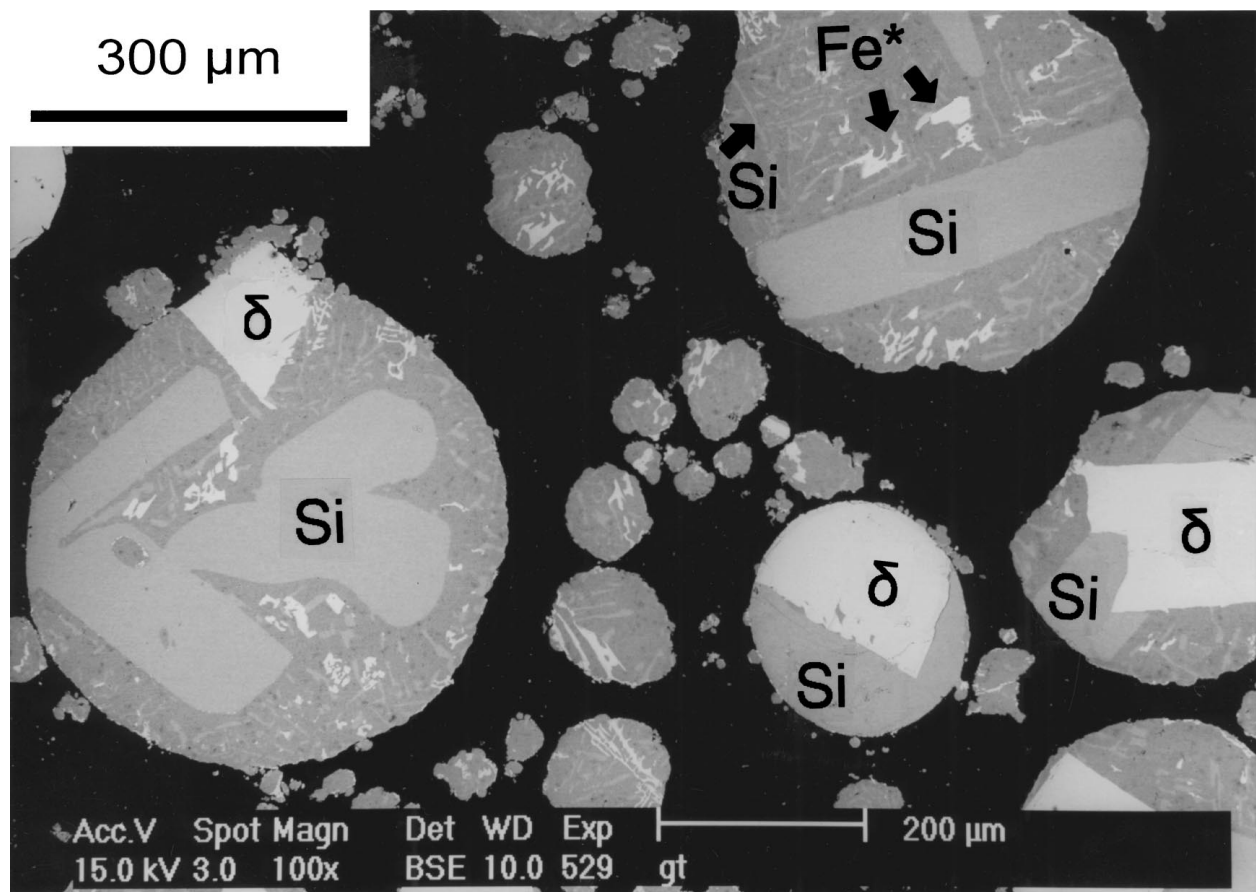
Figure 2 Microstructure of as-atomised powder A (Al-20Si-5Fe-2Ni); Si is not visible in this BSE (Back Scattered Electron) image.

to the temperature of 577 °C of the ternary eutectic $\text{Al} + \text{Si} + \beta \rightarrow \text{L}$ in the Al-Fe-Si system as reported by Rivlin and Raynor [4], or 576 ± 2.5 °C as reported by Petrova and Effenberg [5]. For the present Al-Si-Fe-Ni alloy, the Ni-rich precipitates also appear in this eutectic reaction, lowering the eutectic temperature and leading to the overall reaction $\text{Al} + \text{Si} + \beta + \text{Ni-rich precipitates} \rightarrow \text{L}$. In this case, the ternary equilibrium phase diagram can be used since the low amount of Ni (2 wt%) will only slightly influence the transformations, as will be clarified further. It is found that the transformation temperatures measured by DSC and the accompanying microstructures correspond very well to the transformations in the ternary Al-Fe-Si phase diagram for the present Si and Fe contents. Moreover, during heating of the powder at 5 °C/min, the metastable phases are transformed: Si, which was over-saturated in solid solution, precipitated and the meta-stable δ phase is completely transformed into the stable β phase as illustrated in [9, 10]. The quasi-peritectic* reaction $\beta + \text{Si} \rightarrow \text{L} + \delta$ (peak 2 in Fig. 1) is detected at 589 °C which is again at a slightly lower temperature than the 600 °C temperature reported in [4] and 597 ± 2.5 °C reported in [5] corresponding to the Al-Fe-Si system. The liquidus, characterised by two reactions occurring at almost the same temperature: $\delta + \text{Si} \rightarrow \text{L}$ and $\delta \rightarrow \text{L}$, for the present Fe and Si content is situated at 700 °C in the ternary system. However, it could not clearly be

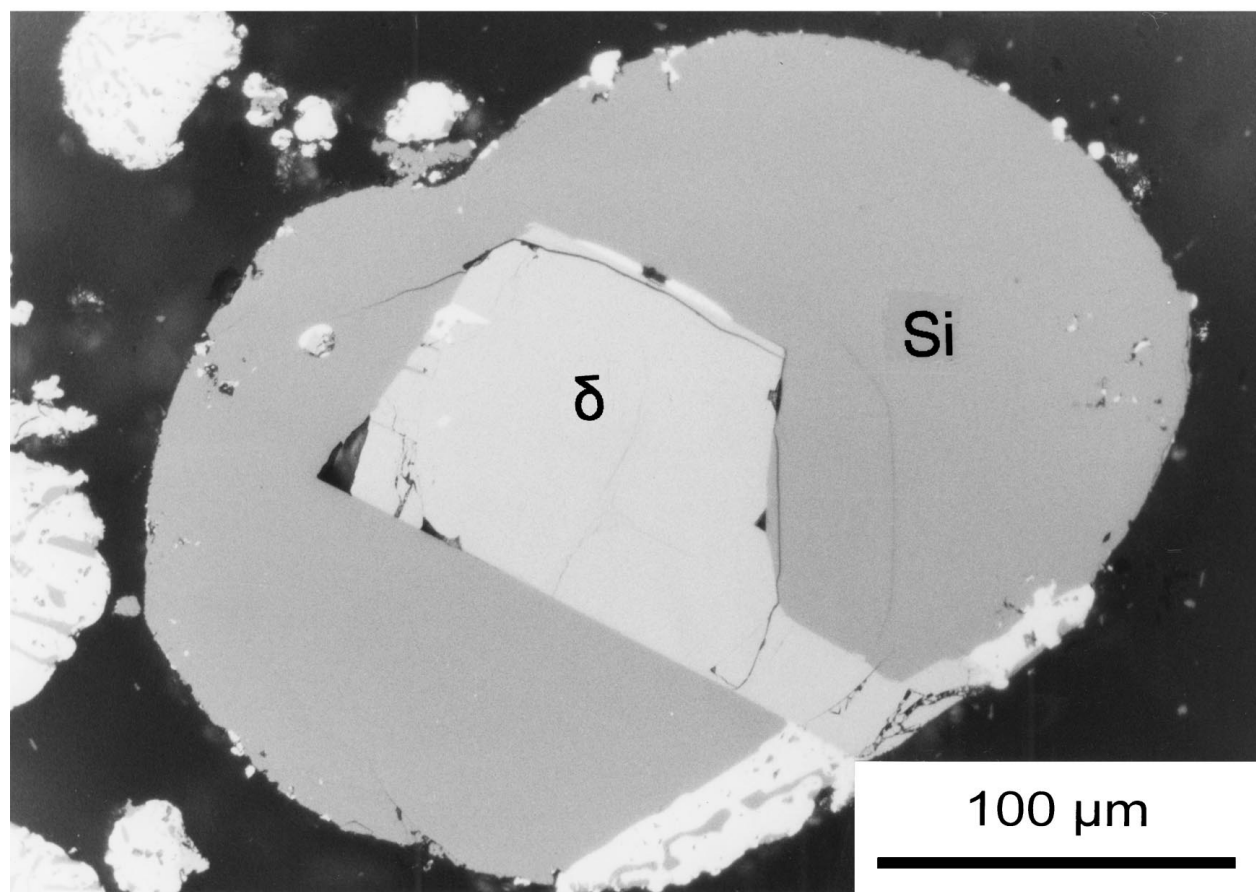
detected in the thermograph. One possible reason can be due to the low amount of heat exchanged, in spite of the high fraction of phases involved. Also, the Si and δ are possibly decomposed gradually (i.e. over a temperature range), which means that no clear transformation peaks are detectable.

During cooling, the primary solidifying phase is δ (Si nucleates at and grows around δ , see Fig. 3). The transformations $\text{L} \rightarrow \delta$ and $\text{L} \rightarrow \delta + \text{Si}$ occur at about 710 °C and are accompanied by an exothermic peak (peak 3 in Fig. 1). The equilibrium transformation temperature may be higher than the measured one caused by undercooling. The ternary quasi-peritectic reaction $\text{L} + \delta \rightarrow \beta + \text{Si}$ does not occur on account of the high cooling rate, as well as attributed to the large diffusion distances required by the large dimensions of the δ phase. The formation of β in this transformation is known to be very slow [4], explained by the so-called enveloping or surrounding effect where, after the first stage of transformation, δ is surrounded by the reaction product β , so that further transformation can only occur by solid state diffusion which is very slow. In the microstructure, it is seen that the β phase is absent after cooling (as was verified by EDS). At 550 °C, the eutectic reaction $\text{L} \rightarrow \text{Al} + \text{Si} + \delta + \text{FeNiAl}_9$ starts (peak 4 in Fig. 1). The eutectic temperature is slightly lower than that defined in the heating part of the cycle, not only due to the undercooling and the thermal inertia, but also due to the different phases involved: δ instead of β , and FeNiAl_9 which might be a different phase than the small Ni-rich precipitates present in the

* The nomenclature ternary quasi-peritectic for the reaction $\text{L} + \delta \leftrightarrow \beta + \text{Si}$ is given in [11].



(a)



(b)

Figure 3 Microstructure of powder A (Al-20Si-5Fe-2Ni) after one thermal cycle; (a) SEM, $Fe^* = FeNiAl_3$, (b) LOM, particle section with almost only δ and Si.

powder. The appearance of FeNiAl₉ at this temperature is in agreement with the observation of the presence of this phase in the forged alloy A, annealed at 550 °C for 3 days [9, 10] indicating that FeNiAl₉ is probably an equilibrium phase.

The microstructure after the first thermal cycle is totally different from that of the starting powder: it is coarse and not very homogeneous as shown by the sections of different powder particles (Fig. 3). The fact that the powder particles are not sintered together, although the microstructure is a typical solidification structure (in comparison with the microstructure obtained after long duration annealing at high temperatures [9, 10]), is attributed to the presence of a strong ductile oxide layer on the surface of the powder particles. This oxide layer prevents sintering of the particles. As is generally known for these Al alloy powders, a special degassing treatment and shearing during hot consolidation is needed to destroy such surface layers [12–14]. The large blocks of δ phase (at% Si/at% Fe = 1.8–2.2 by EDS) are not present in every powder particle section; large primary Si blocks, small eutectic Si, and long and thin irregular FeNiAl₉ are present in every particle section. FeNiAl₉ is often observed at the interface with the δ phase. The measured compositions of the Ni-containing phase (identified by EDS) are within the homogeneity range of FeNiAl₉ [6]. It is possible that the nominal composition slightly varies from one powder particle to another and/or a different type of equilibrium is reached in every particle due to its different particle size. Different powder particle sizes mean different solidification rates during atomisation and thus different metastable microstructures. The microstructure after the first thermal cycle with a low cooling rate of 1 °C/min still contains large δ phases (identified by EDS), indicating that this cooling rate is still too high to form the β phase. The other phases, Si and FeNiAl₉, are identical to those observed in the sample cooled at 5 °C/min.

During the second thermal cycle, the eutectic temperature is 555 °C, which corresponds to the eutectic reaction $\text{Al} + \text{Si} + \delta + \text{FeNiAl}_9 \rightarrow \text{L}$. The quasi-peritectic reaction $\beta + \text{Si} \rightarrow \text{L} + \delta$ does not take place, as there is no β phase formed during the solidification in the first thermal cycle. Moreover, during the second heating no solid state $\delta \rightarrow \beta$ transformation occurred. The reason is that the original very fine microstructure has strongly coarsened so that the diffusion distances for the $\delta \rightarrow \beta$ transformation are increased enormously. There is again no clear heat exchange detected for the last melting reactions. During cooling, the δ and Si phases first solidify at 707 °C (peak 3 in Fig. 1), after which the eutectic reaction $\text{L} \rightarrow \text{Al} + \text{Si} + \delta + \text{FeNiAl}_9$ occurs at 553 °C.

3.2. Forged Al-20Si-5Fe-2Ni (Alloy A)

The DSC curves of forged alloy A are given in Fig. 4. The microstructure of forged alloy A is seen to be as fine as that of the as-atomised powder A, and contains the β (Al₅FeSi) needle-like phase, primary and eutectic Si and small Ni-containing precipitates on the β -needle

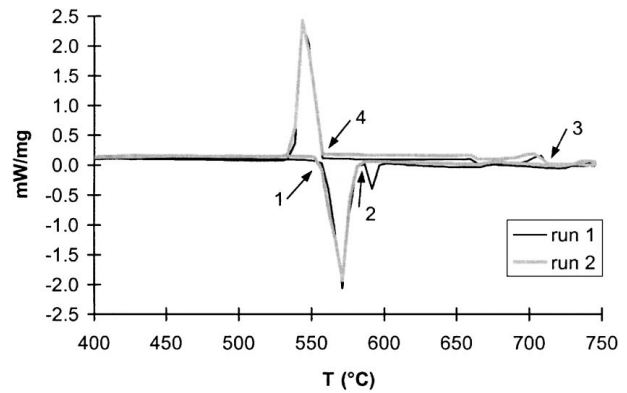


Figure 4 DSC curves of the first and second thermal cycle of forged alloy A (Al-20Si-5Fe-2Ni).

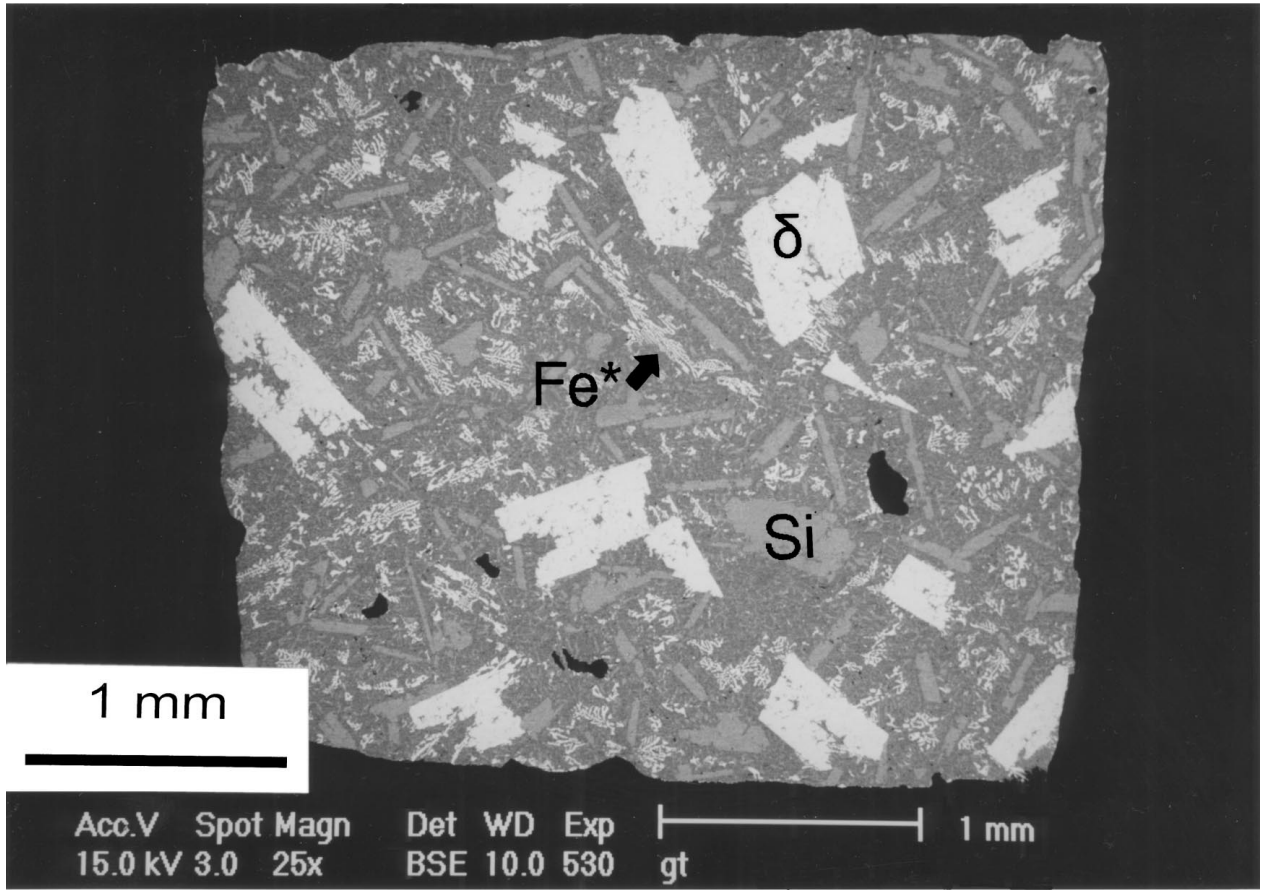
surfaces. Some δ phase may be present in equilibrium with β , Al and Si if the quasi-peritectic transformation is not completely finished [6] although it is not detected by SEM, microanalysis or XRD [9, 10].

During the first heating, the eutectic reaction, $\text{Al} + \text{Si} + \beta + \text{Ni-rich precipitates} \rightarrow \text{L}$ (peak 1 in Fig. 4), occurs at 560 °C, as for the as-atomised powder A. Similarly, the quasi-peritectic reaction $\beta + \text{Si} \rightarrow \text{L} + \delta$ is also observed at 589 °C (peak 2 in Fig. 4). The area of the peak is larger than in the case of powder A, which means that more β is present than in the as-atomised powder at that temperature. This is obvious since the $\delta \rightarrow \beta$ transformation has been (largely) completed during the hot forging at 490 °C. The last solid \rightarrow liquid transformation temperatures are not clearly detected. During cooling, the δ and Si phases first solidify at 713 °C (peak 3 in Fig. 4) and the quasi-peritectic reaction $\text{L} + \delta \rightarrow \beta + \text{Si}$ does not occur for the same reason as that given for powder A. The lowest transformation temperature is for the eutectic at 556 °C. During the heating cycle of the second run, first the eutectic reaction $\text{Al} + \text{Si} + \delta + \text{FeNiAl}_9 \rightarrow \text{L}$ occurs at 556 °C; the quasi-peritectic reaction $\beta + \text{Si} \rightarrow \text{L} + \delta$ again does not occur due to the absence of the β phase. During cooling, the δ and Si phases first appear at 712 °C; finally, the eutectic reaction occurs at 555 °C.

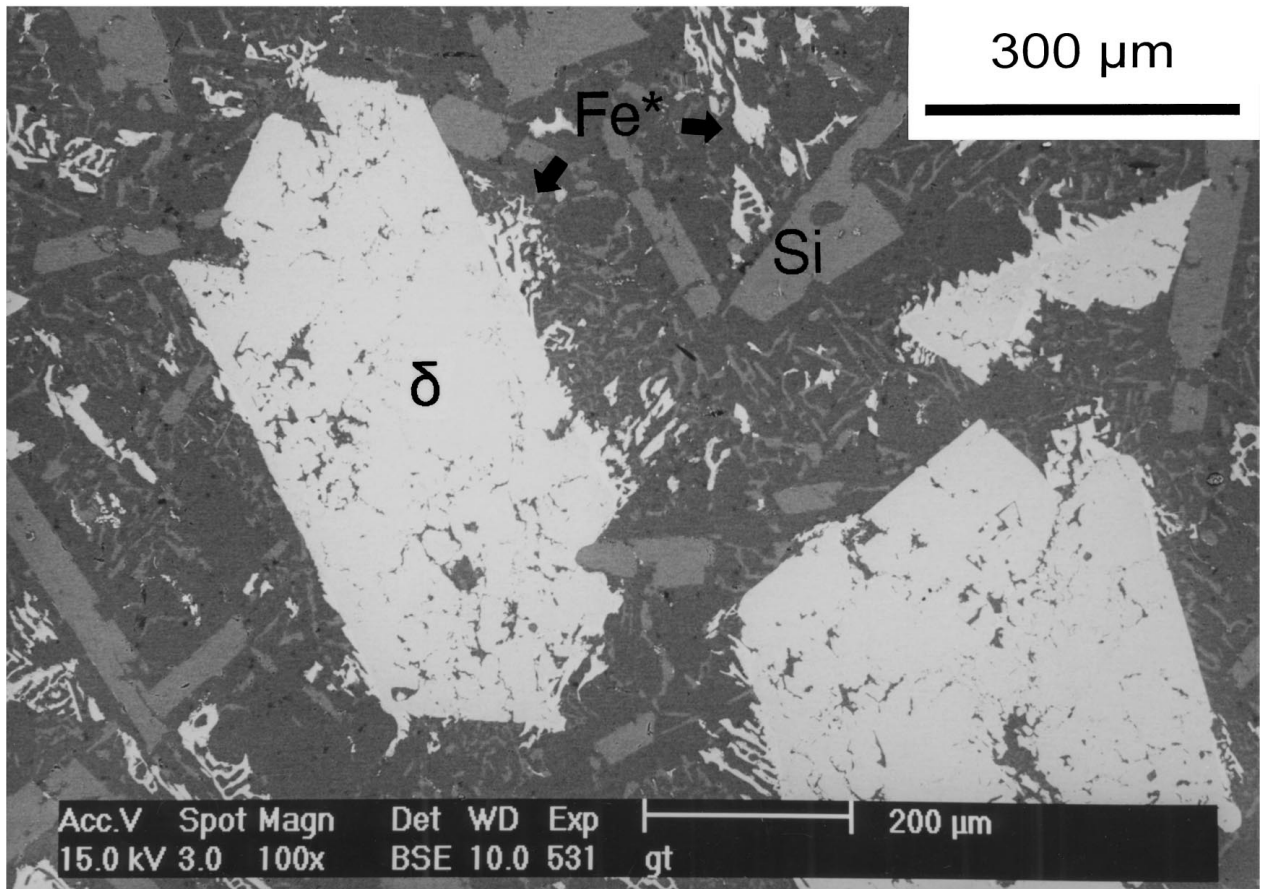
The microstructure obtained after two thermal cycles contains primary δ (at% Si/at% Fe = 2), Si and eutectic FeNiAl₉ (identified by EDS), as in the case of powder A (Fig. 5). After the thermal cycle, the δ blocks in forged alloy A are much larger than those observed in powder A.

3.3. Atomised Al-17Si-5Fe-3.5 Cu-1.1Mg-0.6Zr (Alloy B)

In alloy B a more complex sequence of phase transformations occurs. For this alloy there is no appropriate equilibrium phase diagram available. Therefore, it is not the aim of this study to define complete phase relationships, but to find the temperatures at which phases most probably decompose (from solid to liquid) and form (from liquid to solid), when applying a heating and cooling rate of 5 °C/min. Also incipient (localised) melting is possible due to a non-equilibrium distribution of elements, but this cannot be concluded from this



(a)



(b)

Figure 5 Microstructure of forged alloy A (Al-20Si-5Fe-2Ni) after two thermal cycles; Fe* = FeNiAl₉.

work since the cooling rate might be too high to obtain equilibrium.

In the literature, although several studies about the lowest temperature regarding the solid \leftrightarrow liquid phase transformations in Al-Cu-Mg-Si alloys have been reported, complete transformation schemes have never been defined [7, 8, 15–18]. The reported transformation temperatures strongly depend on the heating and cooling rate and thus on the experimental technique. This may be a reason for the discrepancies in the reported results. A further complication is that the heating/cooling rates are not always given.

Samuel *et al.* [7] reported that, generally, the phases Al_2Cu , Mg_2Si and more complex phases are formed at the end of the solidification, within the temperature interval [520–500 °C] for Al_2Cu and [500–480 °C] for the more complex phases. They studied in detail the dissolution (in the surrounding matrix) and melting of Al_2Cu in a 319.2 type alloy with composition Al-6.2Si-3.2Cu-0.15Fe and confirmed the transformation scheme given in the literature [15] for 319.1 (Al-5.7Si-3.4Cu-0.62Fe-0.36Mn-0.1Mg-0.92Zn-0.14Ti), for a cooling rate of 0.6 °C/min. This scheme states that the $\text{Cu}_2\text{Mg}_8\text{Si}_6\text{Al}_5$ phase (denoted by Q in the reactions below) is the phase last formed (the last 3 reactions are given below):

- 575 °C: $\text{L} \rightarrow \text{Al} + \text{Si} + \beta$
- 525 °C: $\text{L} \rightarrow \text{Al} + \text{Si} + \beta + \text{Al}_2\text{Cu}$ (coarse)
- 507 °C: $\text{L} \rightarrow \text{Al} + \text{Si} + \text{Al}_2\text{Cu}$ (fine) + Q, although Mg_2Si is a possible alternative.

Samuel *et al.* applied a heating rate of 10 °C/min in a DSC and found a similar sequence of transformations at slightly different temperatures in the Mg-free and low Fe-containing alloy (no β nor Q phase):

- 521 °C: Melting (local) of Al_2Cu is expected at temperatures higher than 521 °C; below this temperature Al_2Cu dissolves in the Al matrix.
- 503 °C: Formation of Al_2Cu during cooling.

Yao *et al.* [16] used DTA (Differential Thermal Analysis) at 5 °C/min and directional solidification of the alloy Al-(4.7-4.8)Si-(4.0-4.4)Cu-(0.21-0.56)Fe-(0.48-0.52)Mg-(0-0.28Mn)-(0.012-0.018)Sr. They investigated the reaction scheme reported in [15] and determined the transformation temperatures of the following reactions, in which Al_2Cu is involved:

- 535 °C: $\text{L} \rightarrow \text{Al} + \text{Si} + \text{Al}_2\text{Cu}$
- 485 °C: $\text{L} \rightarrow \text{Al} + \text{Si} + \text{Al}_2\text{Cu} + \text{Q}$

They did not detect the ternary eutectic $\text{L} \rightarrow \text{Al} + \text{Si} + \beta$ nor the β phase because the Fe content of the alloy was too low.

On the other hand, Chakrabarty *et al.* [17] investigated several chill-cast Al-Cu-Mg-Si alloys with DSC (no heating/cooling rate reported) and performed calculations of the phase diagram and solidification using the Scheil model, supposing that eutectic reactions occur. The authors identified a series of localised eutectic melting reactions (monovariant and one invariant)

which occur prior to the bulk solidus melting. During solidification, the Q phase is formed at a higher temperature than the Al_2Cu phase, as is given by the reactions:

- 540 °C: $\text{L} \rightarrow \text{Al} + \text{Q}$
- 510 °C: $\text{L} \rightarrow \text{Al} + \text{Si} + \text{Al}_2\text{Cu} + \text{Q}$

Also the results of Gupta *et al.* [18] indicate that during heating, the Al_2Cu phase decomposes before the Q phase decomposes. They detected insoluble Q phase particles of 1 to 10 μm in Al-1.52Cu-0.75Mg alloy with up to 1.03% Si. Even after 48 h annealing at 530 °C, the Q phase was mainly insoluble. After quenching and extended ageing at 190 °C, the amount of Q phase was not significantly increased.

Finally, Narayanan [8] studied the dissolution of (Al, Fe, Si) phases in a 319 alloy (Al-6.2Si-3.2Cu-0.3Mg-0.15Fe) with increasing Fe content. When cooling at 10 °C/s, the last liquid \rightarrow solid phase transformation occurred at 498 °C and was identified as ‘the eutectic of $\text{Al} + \text{CuAl}_2$ ’. During the solution heat treatment (for 1 h to 1 week solution times), the fine Al_2Cu dissolved at temperatures below 500 °C whereas the coarser Al_2Cu quickly dissolved at temperatures above 500 °C. During a solution treatment at 515 °C the dissolution and fragmentation of the $\beta(\text{Al}_5\text{FeSi})$ was observed. At 535 °C a large interdendritic network of liquid formed, resulting in shrinkage porosity.

In [6] the quinary invariant reactions in the Al-Cu-Fe-Mg-Si system are listed (composition of the alloys is not given). The two invariant reactions at the lowest temperature are: $\text{L} \rightarrow \text{Al} + \text{Cu}_2\text{FeAl}_7 + \text{CuAl}_2 + \text{CuMgAl}_2 + \text{Si}$ and $\text{L} \rightarrow \text{Al} + \text{Cu}_2\text{FeAl}_7 + \text{CuAl}_2 + \text{Mg}_2\text{Si} + \text{Q}$.

For the system Al-Cu-Fe-Si, the following eutectic reaction occurs in high Cu-containing alloys with composition Al-(24-41)Cu-5Fe-5Si and Al-(25-41)Cu-10Fe-11Si: $\text{L} \leftrightarrow \text{Al} + \text{Al}_7\text{Cu}_2\text{Fe} + \text{CuAl}_2 + \text{Si}$ at 520 °C [19].

DSC curves of as-atomised powder B are given in Fig. 6. The initial microstructure of powder B does not significantly differ from that of powder A and contains primary and eutectic Si particles, the needle-like δ phase, and a small amount of Mg-, Fe-, Cu-containing precipitates at the surface of the needles in the super-saturated Al matrix.

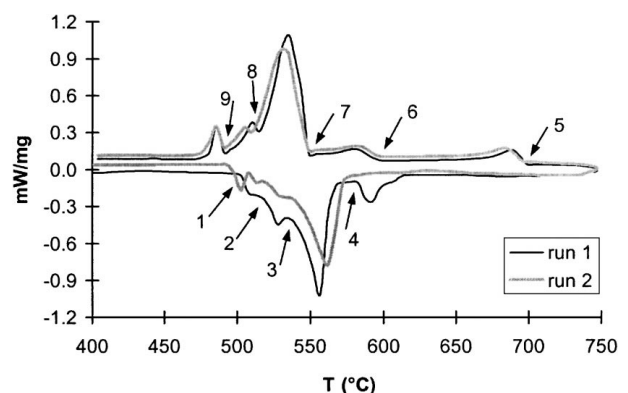
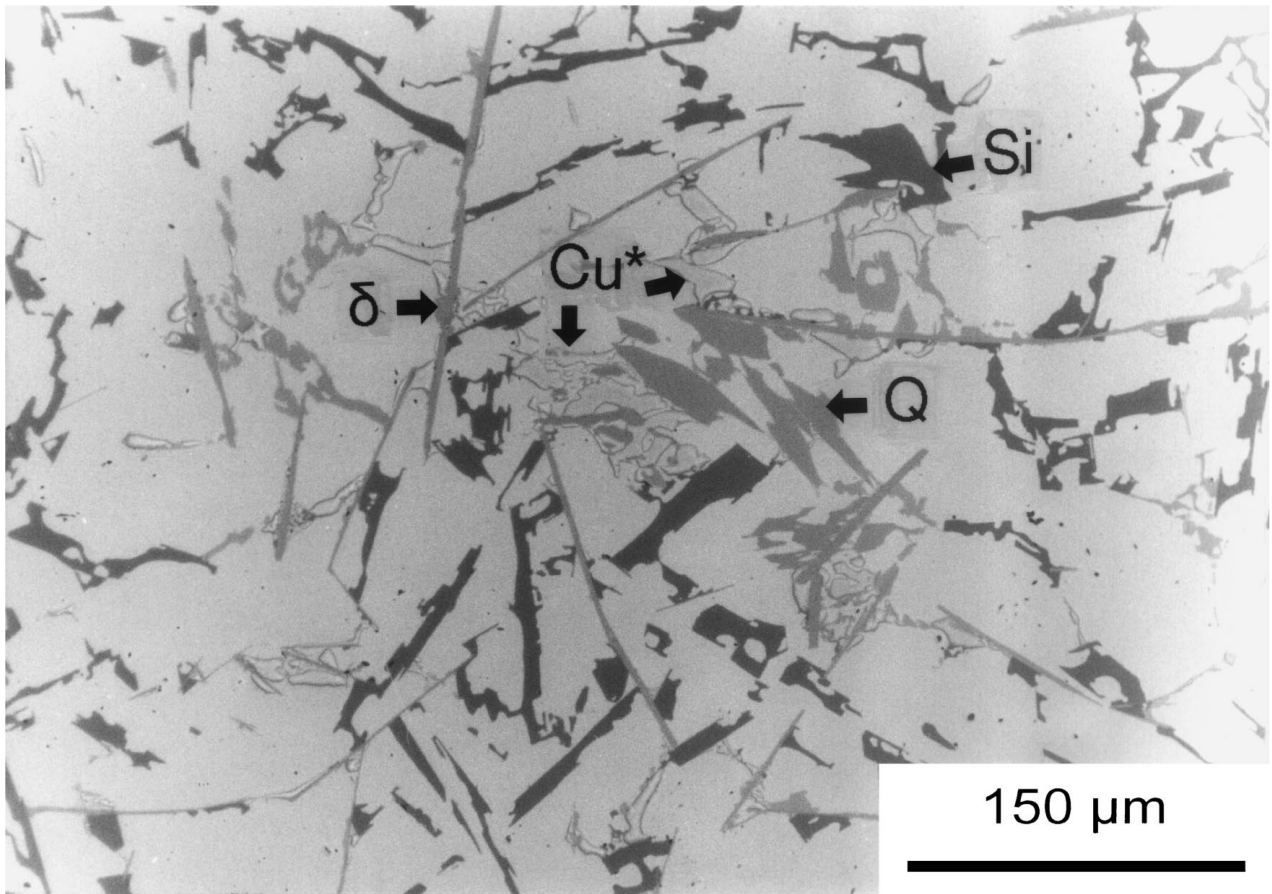
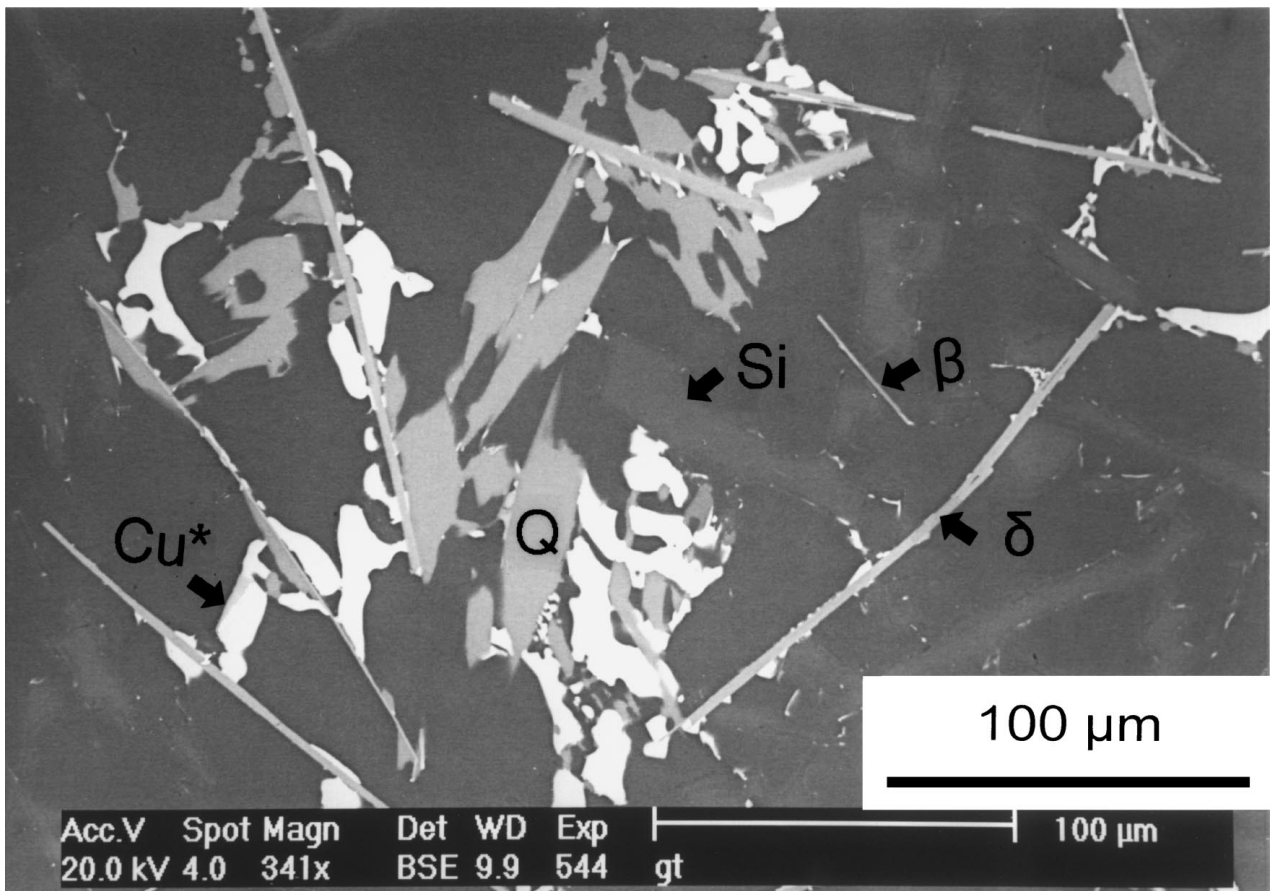


Figure 6 DSC curves of the first and second thermal cycle of powder B (Al-17Si-5Fe-3.5Cu-1.1Mg-0.6Zr).



(a)



(b)

Figure 7 Microstructure of powder B (Al-17Si-5Fe-3.5Cu-1.1Mg-0.6Zr) after two thermal cycles; (a) LOM, (b) SEM; Cu* = Al₂Cu.

During the heating of the first cycle, the solid state transformations are: Si precipitation (200–300 °C), transformation $\delta \rightarrow \beta$ (300–400 °C), precipitation and growth of Cu- and Mg-rich precipitates as $\text{Al}_7\text{Cu}_2\text{Fe}$ and Q ($\text{Al}_5\text{Cu}_2\text{Mg}_8\text{Si}_6$) (from 300 °C) [9, 10].

During the first heating, the temperature at which the first liquid appears, is 505 °C and probably $\text{Al}_7\text{Cu}_2\text{Fe}$ decomposes here (peak 1 in Fig. 6) instead of Al_2Cu as mentioned in [7]. In the next transformation, at about 519 °C, the Q phase is decomposing (peak 2 in Fig. 6). In agreement with the ‘insoluble’ character of Q at 530 °C [18], we can conclude that the first decomposing phase should be $\text{Al}_7\text{Cu}_2\text{Fe}$ and that Q only decomposes at a slightly higher temperature. At about 545 °C a eutectic reaction, corresponding to $\text{Al} + \text{Si} + \beta \rightarrow \text{L}$ in the Al-Si-Fe system, occurs (peak 3 in Fig. 6), probably also involving a reaction of the Cu- and Mg-rich precipitates, resulting in a lower eutectic temperature than for the ternary Al-Si-Fe system (577 °C). Thus, this transformation can be described as $\text{Al} + \text{Si} + \beta + \text{Cu-}, \text{Mg-precipitates} \rightarrow \text{L}$. At 584 °C, a transformation corresponding to the quasi-peritectic reaction $\beta + \text{Si} \rightarrow \text{L} + \delta$ in the Al-Si-Fe system occurs (peak 4 in Fig. 6), in which the Cu- and Mg-rich precipitates are possibly involved. The last decomposition peaks of δ and Si are too weak to be detected.

During cooling and after solidification of δ and Si at about 698 °C (peak 5 in Fig. 6), a small exothermic peak at 596 °C (peak 6 in Fig. 6) is noted, corresponding to the quasi-peritectic reaction $\text{L} + \delta \rightarrow \beta + \text{Si}$. The peak is smaller than that observed during heating, indicating that only a part of the δ is transformed into β . The presence of this peak is in contrast to the results obtained during cooling of powder A, in which no quasi-peritectic reaction occurred. A possible reason can be the effect of Cu and Mg, eventually promoting the quasi-peritectic reaction. The β phase appears as thin needles with a Si/Fe ratio of 1.5 (at%) and not as blocks or as shells around the δ blocks (see below). At 546 °C the eutectic type reaction $\text{L} \rightarrow \text{Al} + \text{Si} + \delta/\beta$, involving probably also Mg- and Cu-rich phases, occurs (peak 7 in Fig. 6). In this transformation, part of the β phase may be formed. At about 514 °C, the Q phase is formed (peak 8 in Fig. 6). The next pronounced peak (9) is situated at a much lower temperature (about 490 °C) than that observed during heating (peak 1) and therefore cannot be attributed to the formation of $\text{Al}_7\text{Cu}_2\text{Fe}$. Accordingly, $\text{Al}_7\text{Cu}_2\text{Fe}$ is absent in the microstructure (confirmed by EDS, see below). Instead of $\text{Al}_7\text{Cu}_2\text{Fe}$, Al_2Cu is formed at that temperature and, indeed, detected in the microstructure (by EDS). This also means that during heating of the atomised powder, it is not Al_2Cu but $\text{Al}_7\text{Cu}_2\text{Fe}$ which is decomposing. The formation of $\text{Al}_7\text{Cu}_2\text{Fe}$ during cooling is not possible because during solidification transformations at higher temperatures all Fe is consumed to form δ and β ; during cooling, the cooling rate is too fast for long distance diffusion to decompose part of the δ and/or β phases to form $\text{Al}_7\text{Cu}_2\text{Fe}$. In the opposite direction, during heating of the powder (see above), the formation of $\text{Al}_7\text{Cu}_2\text{Fe}$ in the solid state from δ and β and dissolved Cu, is associated with

the short diffusion distances in the initial (very fine) microstructure.

During the second heating, at 497 °C, the Al_2Cu phase decomposes first. Thus, the temperature at which the first liquid appears, is lower for alloy B, cooled at 5 °C/min from the liquid state, than for the rapidly solidified (10^4 – 10^6 °C/s) atomised powder. The ‘low temperature melting’ of Al_2Cu is also reported in [7]. The next very small endothermic transformation peak at about 508 °C may be assigned to the decomposition of $\text{Al}_7\text{Cu}_2\text{Fe}$, indicating that a small amount of $\text{Al}_7\text{Cu}_2\text{Fe}$ can be present. Also in the cooling part of the first run, a very small transformation peak is present between peaks 8 and 9, that could confirm this. At 520 °C the Q phase decomposes. At 544 °C, the eutectic type reaction $\text{Al} + \text{Si} + \delta/\beta \rightarrow \text{L}$, involving also Cu- and Mg-rich phases, occurs, probably consuming all the β since at higher temperature, a peak of the quasi-peritectic type reaction $\beta + \text{Si} \rightarrow \text{L} + \delta$ is not observed. During the second cooling, the same transformations and heat exchanges occur as in the first run.

The microstructure obtained after two thermal cycles is given in Fig. 7. Primary δ and Si blocks, eutectic Si needles, eutectic thin δ/β phases, grey Q phase and small white Al_2Cu (at% Al/at% Cu = 2.3–2.5) are present. One can conclude that the formation of $\text{Al}_7\text{Cu}_2\text{Fe}$ is suppressed during solidification at 5 °C/min, because it requires the decomposition of δ and/or β to provide Fe. The Cu is present in the Q phase and in the Al_2Cu phase.

3.4. Forged Al-17Si-5Fe-3.5Cu-1.1Mg-0.6Zr (Alloy B)

The DSC curves of forged alloy B are given in Fig. 8. The microstructure is very fine and contains β needle-like phases, primary and eutectic Si-particles, and small Mg- and Cu-containing precipitates (2.4 to 6 at%) that also contain Si and/or Fe, appearing on the needle surfaces. Some δ phase particles may still be present.

The heating part of the first run is identical to that of powder B. However, the heat content of the decomposition peaks of $\text{Al}_7\text{Cu}_2\text{Fe}$ and Q might be slightly larger than that for powder B, due to a more equilibrium state of the forged material. The cooling part is also identical to that of powder B. However, the quasi-peritectic

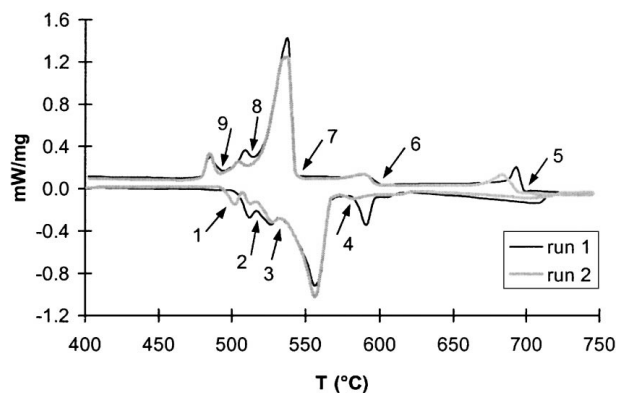
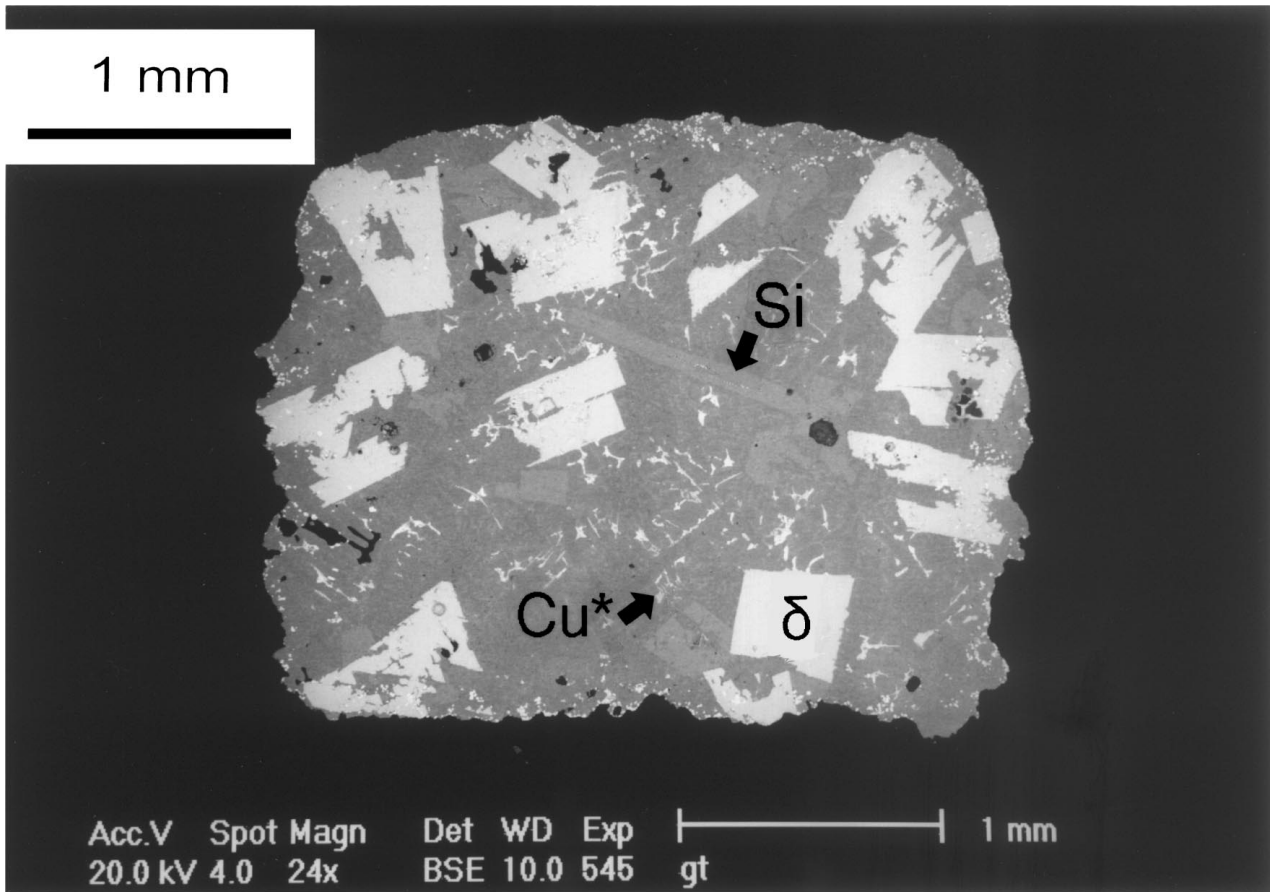
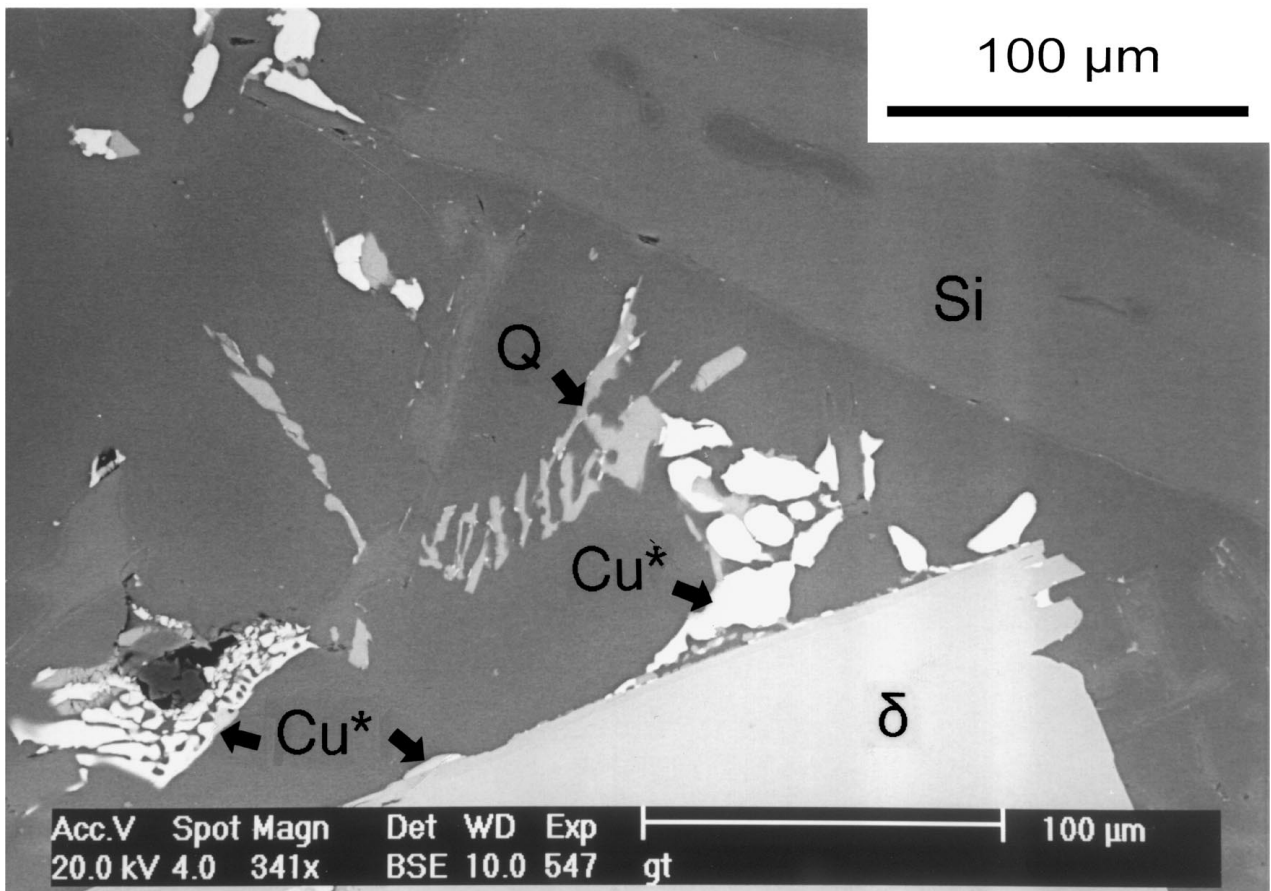


Figure 8 DSC curves of the first and second thermal cycle of forged alloy B (Al-17Si-5Fe-3.5Cu-1.1Mg-0.6Zr).



(a)



(b)

Figure 9 Microstructure of forged alloy B (Al-17Si-5Fe-3.5Cu-1.1Mg-0.6Zr) after two thermal cycles; Cu* = Al₂Cu.

type reaction peak $L + \delta \rightarrow \beta + Si$ is slightly larger than for powder B, meaning that more β is formed during solidification of forged B. The heating part of the second run is identical to that of powder B. The decomposition peak of Al_2Cu is somewhat larger and the quasi-peritectic type reaction peak $\beta + Si \rightarrow L + \delta$ is very small. The results for the cooling part of the second run are in general similar to those of the first thermal cycle.

The microstructure of forged B after two thermal cycles is shown in Fig. 9 and contains the same phases (as identified by EDS) as those observed in powder B heat treated similarly.

4. Conclusions

Using high temperature DSC, microscopy, EDS microanalysis and XRD, the metastable and stable solid \leftrightarrow liquid phase transformations in metastable powder and forged Al-Si-Fe-Ni and Al-Si-Fe-Cu-Mg-Zr alloys have been identified, for a heating and cooling rate of 5 °C/min and 1 °C/min. The results are summarised in Tables I and II. Processing parameters for hot forging and heat treatments are restricted by the temperature at which the first liquid appears, which is 559 °C for the powder and 560 °C for the forged alloy Al-20Si-5Fe-2Ni and 505 °C for the powder and 506 °C for the forged alloy Al-17Si-5Fe-3.5Cu-1.1Mg-0.6Zr.

Further, in the Al-17Si-5Fe-3.5Cu-1.1Mg-0.6Zr alloy the Al_7Cu_2Fe phase decomposes at the lowest temperature during melting. This can be utilised during a heat treatment with local melting to increase the amount of Cu dissolved in the Al matrix prior to quenching. However, there is a risk of pore formation and formation of brittle Cu-containing phases, so that it is necessary to verify the possible positive effect on the mechanical properties.

Finally, the report in some references that the Q phase ($Cu_2Mg_8Si_6Al_5$) is the first decomposing phase during melting, is not confirmed for the hypereutectic Cu-, Mg-containing alloy investigated in the present study.

Acknowledgements

The authors are grateful to Dr. H. Kumar and Professor L. Delaey (MTM, K. U. Leuven) for a critical reading of the manuscript, and for financial support from the European Commission, since part of this work was un-

dertaken within the framework of the BRITE-project BRE2 CT92 0220.

References

1. J. L. ESTRADA and J. DUSZCZYCK, *Journal of Materials Science* **25** (1990) 886.
2. J. ZHOU and J. DUSZCZYCK, *ibid.* **27** (1992) 3856.
3. J. L. ESTRADA and J. DUSZCZYCK, *ibid.* **25** (1990) 1381.
4. V. G. RIVLIN and G. V. RAYNOR, *International Metals Review* **3** (1981) 133.
5. L. A. PETROVA and G. EFFENBERG, in "Red Book, Vol. 37, Part 1: Phase Diagrams of Metallic Systems (Summaries of the Publication year 1992)" (MSI, Materials Science International GmbH, Stuttgart, Germany, 1997) p. 395.
6. L. F. MONDOLFO, in "Aluminum Alloys: Structure and Properties" (Butterworths, London/Boston, 1976).
7. A. M. SAMUEL, J. GAUTHIER and F. H. SAMUEL, *Metallurgical and Materials Transactions A* **27A** (1996) 1785.
8. L. A. NARAYANAN, F. H. SAMUEL and J. E. GRUZLESKI, *ibid.* **26A** (1995) 2161.
9. G. TIMMERMANS and L. FROYEN, in Proceedings of the European Conference on Advanced PM Materials, Vol. 1, Birmingham, October 1995, edited by the European Powder Metallurgy Association (European Powder Metallurgy Association, 1995) p. 224.
10. G. TIMMERMANS, PhD Thesis, Department of Metallurgy and Materials Engineering, Katholieke Universiteit Leuven, 2000.
11. A. PRINCE, in "Alloy Phase Equilibria" (Elsevier Publishing Company, Amsterdam/London/New York, 1966) p. 173.
12. J. L. ESTRADA and J. DUSZCZYCK, *Journal of Materials Science* **26** (1991) 1431.
13. *Idem.*, *ibid.* **26** (1991) 3909.
14. L. KOWALSKI, B. M. KOREVAAR and J. DUSZCZYCK, *Journal of Materials Science* **27** (1992) 2770.
15. L. BÄCKERUD, G. CHAI and J. TAMMINEN, in "Solidification Characteristics of Al Alloys, Vol. 2: Foundry Alloys" (AFS/SKANALUMINIUM, Des Plaines, IL, 1990) p. 71.
16. J.-Y. YAO, G. A. EDWARDS, L.-H. ZHENG and D. A. GRAHAM, in "Aluminium Alloys; Their Physical and Mechanical Properties, Part 1," edited by J. H. Driver, B. Dubost, F. Durand, R. Fougères, P. Guyot, P. Sainfort and M. Suery (TransTech Publications, Switzerland/Germany/UK/USA, 1996) p. 183. Proceedings of the 5th International Conference ICAAS, Grenoble, July, 1996.
17. D. J. CHAKRABARTI and J. L. MURRAY, *ibid.* p. 177.
18. A. K. GUPTA, A. K. JENA and M. C. CHATUVERDI, *Materials Science and Technology* **3** (1987) 1012.
19. L. A. PETROVA and G. EFFENBERG, in "Red Book, Vol. 35, Part 2: Phase Diagrams of Metallic Systems (published in 1990)" (MSI, Materials Science International GmbH, Stuttgart, Germany, 1993) p. 711.

Received 26 May

and accepted 16 December 1999